

**AN EVALUATION OF TECHNIQUES USED IN THE AGE AND PETROLOGIC ANALYSIS OF APOLLO 12 BASALTS.** J. F. Snape<sup>1</sup>, S. Beaumont<sup>2</sup>, R. Burgess<sup>3</sup>, I. A. Crawford<sup>1</sup>, and K. H. Joy<sup>1,4,5</sup>, <sup>1</sup>CPS at UCL-Birkbeck, London, UK ([j.snape@ucl.ac.uk](mailto:j.snape@ucl.ac.uk)), <sup>2</sup>Ecole et Observatoire des Sciences de la Terre, Université De Strasbourg, France, <sup>3</sup>SEAES, University of Manchester, Manchester, UK, <sup>4</sup>The Center for Lunar Science and Exploration, The Lunar and Planetary Institute, USRA, Houston 77058, USA, <sup>5</sup>The NASA Lunar Science Institute.

**Introduction:** The Apollo 12 mission returned a collection of predominantly low-Ti ( $\text{TiO}_2 = 1\text{-}6 \text{ wt.}\%$ ) basaltic rocks from the southeastern region of Oceanus Procellarum [1]. We are analyzing a selection of Apollo 12 regolith particles, in an attempt to better characterize the diversity of basaltic flows at the landing site [2]. We are using a multi-technique approach that is initially being tested on several previously well-studied Apollo 12 basalt fragments. Here we will focus primarily on our results for the sample 12038, but also give modal mineralogies and bulk compositions for two other samples, 12022 and 12063 (Tables 1 and 2).

**Methods:** Small fragments of 12038,263 were subdivided for combined chemical petrologic and age studies. A JEOL JXA-8100 electron microprobe (EMP) with an accompanying Oxford Instruments EDS probe and INCA software package was used to acquire back scattered electron (BSE) images (Fig. 1a), elemental maps (Fig. 1b) and bulk sample compositions. Modal mineralogies were obtained from the BSE images and element maps by using the GNU Image Manipulation Program (GIMP) to count the pixels associated with each phase (Table 1). The bulk sample compositions were measured by performing multiple raster beam analyses (RBA) across the sample areas. These values were corrected for differing phase densities (following the method of [3]) and averaged; the resulting standard deviations indicate their reproducibility (Table 2). A small portion of each sample was used for laser stepped heating Ar-Ar age determinations.

**Sample descriptions:** 12038 is the only sample classified as a feldspathic basalt [e.g. 4,5,6] as it has

more feldspar and higher concentrations of Na, Al and REE than other Apollo 12 basalts [7]. 12022 and 12063 are both classified as ilmenite basalts [4].

**12038,263.** As previously reported for other samples of 12038 [4,6] this particular sample has a subophitic texture with a grain size of 0.1-1.0 mm (Fig. 1). It consists mostly of pyroxene (49.7% by area) and plagioclase (44.0%). The pyroxene phases show prominent zonation from their cores to rims (Fig. 1). Also present are elongated grains of ilmenite and small (<0.1 mm) anhedral crystals of a silica polymorph (possibly cristobalite [6]). Neal et al. [1] identified a minor (0.1%) olivine component in 12038, however, probably due to the small sample size olivine was not observed in our sub-section.

**Ar-Ar dating:** Previously Rb/Sr and Nd/Sm isochron ages of 3.28 and 3.35 Ga have been obtained for 12038 by [7,8]. We obtained Ar-isotope data from two whole-rock samples which give an age of  $3.14 \pm 0.04$  Ga based on the final 20-30%  $^{39}\text{Ar}$  released (Fig. 2). This is indistinguishable from the Ar-Ar age of 3.1 Ga obtained from a 100x larger mass sample of 12038 [9]. We attribute the somewhat lower Ar-Ar age to  $^{40}\text{Ar}$  loss manifested by the pattern of increasing apparent ages in the age spectra (Fig 2).  $^{40}\text{Ar}$  loss most likely occurred by impact heating  $\leq 1\text{Ga}$ . Similar ages have been obtained for several other Apollo 12 basalts (e.g. 12008; 12009; 12017; 12051) by Ar-Ar dating [4] possibly suggesting a common reset age.

We have also obtained a cosmic-ray exposure (CRE) age of  $180 \pm 2$  Ma from the sample. Given uncertainties in cosmogenic  $^{38}\text{Ar}$  production rate we regard this to be in broad agreement with  $230 \pm 15$  Ma as rec-

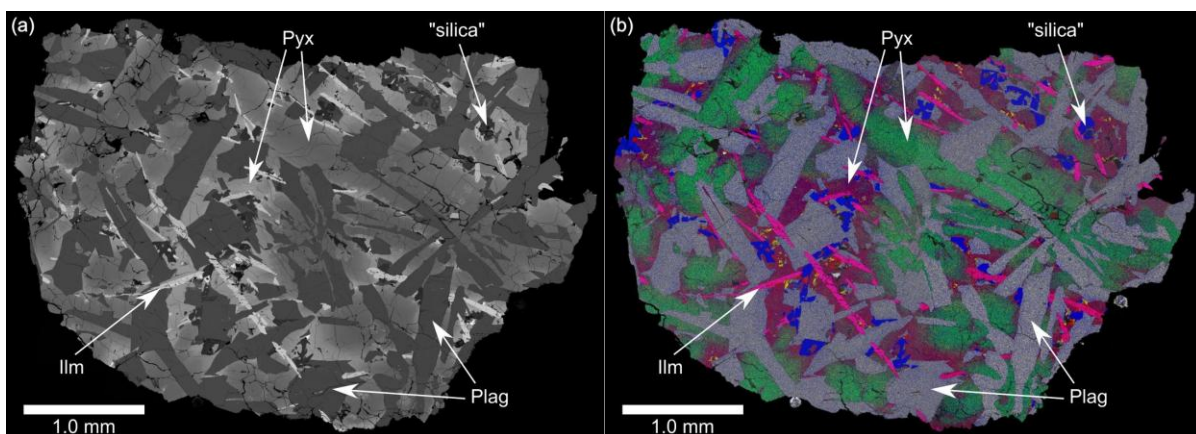


Figure 1: (a) BSE image of 12038,263. (b) Montaged false color elemental map of 12038,263 where colors represent element concentrations: Si = blue, Al = white, Mg = green, Fe = red, Ca = yellow and Ti = pink.

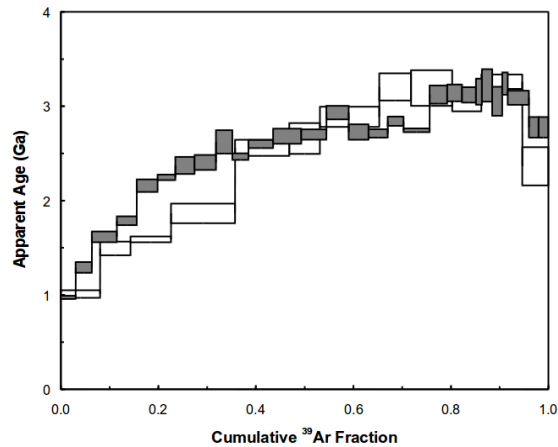


Figure 2: Apparent age of 12038,263 sample, during laser stepped heating.

ordered by [4]. The similar exposure ages obtained for a number of other Apollo 12 basalts (e.g. 12002; 12018; 12064) may suggest that a single impact event was responsible for exposing all of these samples [4].

**Discussion:** The techniques used for establishing modal mineralogy, bulk composition and age of this sample have produced results which are broadly comparable with those reported previously which were often obtained using much larger samples. Some discrepancies are observed between our results and those of previous studies. For example, we obtain a higher abundance of plagioclase and lower abundance of pyroxene in our sample of 12022, and to a lesser extent 12063. However, this can be explained by the use of

small (<1 cm surface area studied) sub-samples of the parent rocks (c.f. Table 1). The lower abundance of pyroxene also explains the lower bulk MgO values within these samples. This observation highlights the higher uncertainties associated with data obtained from small (especially coarse-grained) samples which may not necessarily be representative of their parent rock. Nevertheless, the broad agreement with previous studies indicates that the approach used here is appropriate for investigating unstudied fines (1-2 mm chips) which are currently being studied as part of our basalt diversity project (see [2]).

**Acknowledgements:** We thank CAPTEM for sample allocation and the staff of the Lunar Sample Curation Facility at NASA JSC for their expert assistance in the selection and processing of these samples. Funding from STFC is gratefully acknowledged.

**References:** [1] Neal et al. (1994) *Meteoritics*, 29, p334–348. [2] Snape et al. (2011) *LPS, XLII*, this meeting. [3] Warren (1997) *LPS, XXVIII*, Abstract #1497. [4] Meyer C. (2005) *Lunar Sample Compendium*, <http://curator.jsc.nasa.gov/lunar/compendium.cfm>. [5] Keil K. et al. (1971) *LPS, II*, p319–341. [6] Beaty D. W. et al. (1979) *LPS, X*, p359–463. [7] Nyquist L. E. (1981) *Earth Planet. Sci. Lett.*, 55, p335–355. [8] Compston W. et al. (1971) *LPS, II*, p1471–1485. [9] Turner G. (1977) *Phys. Chem. Earth*, 10, p145–195. [10] Brett et al. (1971) *LPS, II*, p301–317. [11] Taylor et al. (1971) *LPS, II*, p1939–1948. [12] LSPET (1970) *Science*, 167, p1325–1339. [13] Kushiro and Haramura (1971) *Science*, 171, p1235–1237. [14] Willis et al. (1971) *LPS, II*, p1123–1138. [15] Wakita and Schmitt (1971) *LPS, II*, p1231–1236.

	12038			12022			12063		
	This study	[6] Beaty et al. (1979)	[1] Neal et al. (1994)	This study	[10] Brett et al. (1971)	[1] Neal et al. (1994)	This study	[11] Taylor et al. (1971)	[1] Neal et al. (1994)
Olivine	-	-	0.1	15.8	16.5	19.5	6.4	7.8	2.8
Pyroxene	49.7	49.0	48.8	47.2	58.6	56.0	54.3	56.8	64.6
Plagioclase	44.0	44.0	43.8	28.0	12	12.2	32.9	27.1	21.6
Opauques	3.5	3.7	3.7	5.4	11.2	9.0	5.8	4.8	8.0
“Silica”	2.8	2.7	2.7	3.6	-	0.2	0.6	2.0	0.1
Other (e.g. mesostasis)	-	0.1	-	-	1.6	2.3	-	-	2.5

Table 1: Modal mineralogy of 12038, 12022 and 12063. We have compared our values with those of [1,6,10,11] which were acquired using point counting techniques.

	12038				12022			12063		
	This study	[12] LSPET (1970)	[13] Kushiro and Haramura (1971)	[8] Compston et al. (1971)	This study	[12] LSPET (1970)	[13] Kushiro and Haramura (1971)	This study	[14] Willis et al. (1971)	[15] Wakita and Schmitt (1971)
Na <sub>2</sub> O	0.86 ± 0.01	0.60	0.64	0.66	0.46 ± 0.01	0.36	0.29	0.47 ± 0.01	0.31	0.28
MgO	5.95 ± 0.03	6.50	7.09	6.71	8.95 ± 0.04	13.00	11.58	8.93 ± 0.04	9.56	11.40
Al <sub>2</sub> O <sub>3</sub>	13.95 ± 0.05	12.00	12.12	12.53	9.85 ± 0.02	11.00	9.12	11.05 ± 0.02	9.27	9.10
SiO <sub>2</sub>	46.79 ± 0.06	49.00	47.05	46.56	43.18 ± 0.07	36.00	42.33	43.43 ± 0.07	43.48	42.80
P <sub>2</sub> O <sub>5</sub>	0.32 ± 0.02		0.02	0.14	0.21 ± 0.02		0.02	0.19 ± 0.02	0.14	
SO <sub>3</sub>	0.26 ± 0.02			0.06	0.41 ± 0.02			0.27 ± 0.03	0.09	
K <sub>2</sub> O	0.09 ± 0.01	0.06	0.07	0.07	0.08 ± 0.01	0.07	0.07	0.06 ± 0.01	0.06	
CaO	11.03 ± 0.03	11.00	11.46	11.62	9.39 ± 0.03	11.00	9.37	10.14 ± 0.03	10.49	10.80
TiO <sub>2</sub>	3.35 ± 0.04	3.20	3.22	3.31	5.44 ± 0.04	5.10	4.54	4.87 ± 0.04	5.00	5.00
Cr <sub>2</sub> O <sub>3</sub>	0.26 ± 0.02	0.32	0.34	0.27	0.38 ± 0.03	0.39	0.56	0.41 ± 0.02	0.44	0.41
MnO	0.22 ± 0.02	0.26	0.24	0.27	0.25 ± 0.01	0.17	0.26	0.25 ± 0.01	0.28	0.27
FeO	16.95 ± 0.08	17.00	17.91	17.99	21.41 ± 0.07	22.00	22.06	19.91 ± 0.04	21.26	21.20
Total	100.00	99.94	100.16	100.19	100.00	99.09	100.20	100.00	100.38	101.25
Mg#	38.49	40.55	41.39	39.95	42.71	51.32	48.36	44.46	44.51	48.96
Analytical method	EMP RBA	optical spectrographic techniques	conventional wet chemistry	XRF	EMP RBA	optical spectrographic techniques	conventional wet chemistry	EMP RBA	XRF	INAA

Table 2: Normalized bulk composition of 12038, 12022 and 12063. These values were averaged from 5 sets of measurements per sample. The errors provided are the 1σ standard deviations of these measurements. We have compared our data with those of [8,12,13,14,15].